

PHYLOGENETIC ANALYSIS OF *BRACHIDINIUM CAPITATUM* (DINOPHYCEAE) FROM THE GULF OF MEXICO INDICATES MEMBERSHIP IN THE KARENIACEAE¹

Darren W. Henrichs

Department of Biology, Texas A&M University, College Station, Texas 77843, USA

Heidi M. Sosik, Robert J. Olson

Department of Biology, Woods Hole Oceanographic Institution, Woods Hole, Massachusetts 02543, USA

and Lisa Campbell²

Department of Oceanography and Department of Biology, Texas A&M University, College Station, Texas 77843, USA

Brachidinium capitatum F. J. R. Taylor, typically considered a rare oceanic dinoflagellate, and one which has not been cultured, was observed at elevated abundances (up to 65 cells · mL⁻¹) at a coastal station in the western Gulf of Mexico in the fall of 2007. Continuous data from the Imaging FlowCytobot (IFCB) provided cell images that documented the bloom during 3 weeks in early November. Guided by IFCB observations, field collection permitted phylogenetic analysis and evaluation of the relationship between *Brachidinium* and *Karenia*. Sequences from SSU, LSU, internal transcribed spacer (ITS), and *cox1* regions for *B. capitatum* were compared with five other species of *Karenia*; all *B. capitatum* sequences were unique but supported its placement within the Kareniaceae. From a total of 71,487 images, data on the timing and frequency of dividing cells was also obtained for *B. capitatum*, allowing the rate of division for *B. capitatum* to be estimated. The maximum daily growth rate estimate was 0.22 d⁻¹. Images showed a range in morphological variability, with the position of the four major processes highly variable. The combination of morphological features similar to the genus *Karenia* and a phylogenetic analysis placing *B. capitatum* in the *Karenia* clade leads us to propose moving the genus *Brachidinium* into the Kareniaceae. However, the lack of agreement among individual gene phylogenies suggests that the inclusion of different genes and more members of the genus *Karenia* are necessary before a final determination regarding the validity of the genus *Brachidinium* can be made.

Key index words: *Brachidinium*; *cox1*; dinoflagellate; flow cytometry; Gulf of Mexico; ITS; *Karenia*; LSU; phylogeny; SSU

Abbreviations: BI, Bayesian inference; *cox1*, cytochrome c oxidase I; IFCB, Imaging FlowCytobot;

ITS, internal transcribed spacer; ML, maximum likelihood; MP, maximum parsimony

Members of the genus *Brachidinium* have been observed in samples from throughout the world, yet they remain poorly known because they have always been recorded at extremely low abundances. The type species, *B. capitatum*, originally described by Taylor (1963) from the southwest Indian Ocean, has also been identified from the Pacific Ocean (Hernandez-Becerril and Bravo-Sierra 2004, Gomez 2006), the northeast Atlantic Ocean, the Mediterranean Sea (Gomez et al. 2005b and references therein), and, most recently, the Gulf of Mexico (this study).

The genus *Brachidinium* currently includes four species: *B. capitatum*, *B. catenatum* F. J. R. Taylor (Taylor 1966), *B. brevipes* Sournia (Sournia 1972), and *B. taylorii* Sournia (Sournia 1972). *B. capitatum* is characterized by the presence of four movable processes originating from the cell body (Gomez et al. 2005b), a length of 31–46 μm (including ventral processes), and a width of 95–123 μm (including the lateral processes; Taylor 1963). *B. catenatum* was described as a chain-forming species with a length of 30–45 μm (including ventral processes) and chains being 28–32 μm in width (Taylor 1966). *B. brevipes* is a smaller cell, relative to the type species, with a length of ~25–30 μm (including ventral processes; estimated from fig. 4 in Sournia 1972), a width of ~68 μm (including lateral processes), and triangular antapical processes, wider at the base and tapering to a point (Sournia 1972). *B. taylorii* is also a smaller cell, but morphologically very similar to the type species. It has a length of ~25 μm (including antapical processes; estimated from fig. 3 in Sournia 1972) and a width of ~68 μm (including the lateral processes; estimated from fig. 3 in Sournia 1972). The taxonomic framework we use here follows Sournia (1986) and incorporates the

¹Received 2 June 2010. Accepted 6 October 2010.

²Author for correspondence: e-mail lcampbell@ocean.tamu.edu.

modification of Gomez et al. (2005a) eliminating the order Brachidinales and moving the family Brachidiaceae into the Gymnodinales. The genus *Brachidinium* is one of two genera (the other being *Asterodinium*) in the family Brachidiaceae.

After the original description of the type species, it was suggested that members of the Brachidinales may be life-cycle stages of other dinoflagellate species (Sournia 1986 per Gomez et al. 2005a). Gomez et al. (2005a) noted that cells of both *Brachidinium* and *Asterodinium*, a closely related genus in the Brachidiaceae, exhibited a high morphological variability and co-occurred with cells resembling members of the genus *Karenia*. A detailed morphological description of *B. capitatum* provided by Gomez et al. (2005b) was used to support the idea that members of the Brachidinales were life-history stages of *Karenia* spp., specifically *K. papilionacea* Haywood et Steid. In addition, the validity of other species in the genus *Brachidinium* has recently been questioned (Gomez et al. 2005b). Two species, *B. catenatum* (Taylor 1966) and *B. brevipes* (Sournia 1972), have not been reported since their original descriptions, which led Gomez et al. (2005b) to suggest that these other described species of *Brachidinium* may simply be morphological variants of the type species. Taylor (1966) noted during his original description of *B. catenatum* that it might simply be a small neritic or summer form of *B. capitatum*. Gomez et al. (2005a) went further in recommending the elimination of the order Brachidinales based on the lack of a difference between some morphological characters of *Brachidinium* spp. and *Karenia* spp. Genetic sequence data from *B. capitatum* would be helpful in determining the appropriate phylogenetic placement of the genus *Brachidinium* and answering the question of whether *B. capitatum* is a life-history stage of *K. papilionacea*.

A phytoplankton time series in the Gulf of Mexico at Port Aransas, Texas, utilizing the IFCB (Olson and Sosik 2007) has provided nearly continuous data since fall 2007 (Campbell et al. 2010). The temporal resolution from continuous sampling and automated analysis of a large number of images (Sosik and Olson 2007) allows us to estimate cell size, timing of division, and growth rate (Campbell et al. 2010). Here, we report observations of *B. capitatum* for a period of ~ 3 weeks beginning in October 2007. This rare species has not been cultured successfully, and consequently, little information is available about the life cycle of *B. capitatum*. Guided by IFCB observations, field collection permitted phylogenetic analysis and evaluation of the relationship between *Brachidinium* and *Karenia*. This time series also provided data on the timing and number of dividing cells, from which the rate of division for *B. capitatum* could be estimated. We report here the first observed "bloom" of *B. capitatum* in the Gulf of Mexico, an ~ 3-week event during the fall of 2007 when concentrations at times exceeded 50 cells · mL⁻¹.

MATERIALS AND METHODS

Sample collection and cell isolation. The bloom of *B. capitatum* began in late October 2007. A water sample collected on 14 November 2007 from the University of Texas Marine Science Institute (UTMSI) in Port Aransas, Texas (27.84° N, 97.07° W), was preserved with Lugol's iodine, refrigerated at 4°C, and used for DNA extraction. The single-cell PCR protocol of Henrichs et al. (2008) was used with the following modification. The first 25 cells identified as *B. capitatum* were isolated into five separate 0.2 mL PCR tubes (five cells per tube) to increase the amount of template DNA available for amplification. External morphology of all cells was very similar, and there was no discrimination of cells based on the position of the four major processes. All tubes were centrifuged briefly and subjected to three rounds of freezing and thawing to lyse the cells and allow further DNA amplification (Henrichs et al. 2008).

Culture DNA extraction. Cell pellets from cultures of *Karenia bidigitata* Haywood et Steid. (= *K. bicuneiformis*; strain: CAWD92); *K. papilionacea* (strain: CAWD91); *K. selliformis* Haywood, Steid. et Mack. (strain: CAWD79); and *Takayama acrotrocha* (J. Larsen) de Salas, Bolch et Hallegr. (strain: MC728-D5) were subjected to cetyltrimethyl ammonium bromide (CTAB) DNA extraction (Doyle and Doyle 1990), rehydrated with 1X Tris-EDTA (1XTE) solution, and used as template for whole genome amplification. The culture pellet of *T. acrotrocha* was generously provided by Raffaele Siano (Stazione Zoologica Anton Dohrn). Cultures of *K. bidigitata*, *K. papilionacea*, and *K. selliformis* were acquired from the Cawthron Institute Collection of Micro-algae (CICCM; <http://cultures.cawthron.org.nz>). We use the name *K. bidigitata* here to maintain consistency with the CICCM, whose culture we sequenced and which was described by Haywood et al. (2004).

DNA amplification, purification, and sequencing. The lysate in each tube was used as template for a whole genome amplification reaction (Genomiphi, GE Healthcare, Little Chalfont, UK). DNA extracted from cultures was amplified in an identical manner. The whole genome amplification reaction was carried out according to the kit protocol. The resulting product was diluted with 180 µL of 1XTE solution and used as template for subsequent PCR. The following were amplified using 50 µL reactions: (i) the SSU (primers: 18SA and 18SB from Medlin et al. 1988, primers: 1055F and 1055R from Elwood et al. 1985); (ii) LSU (D1/D2 region; primers: D1R and D2C from Scholin et al. 1994); (iii) ITS regions of the ribosomal genes ITS 1 and ITS 2, including the 5.8S region (primers: ITS1 and ITS4 from White et al. 1990); and (iv) the mitochondrial *cox1* (primers: DinoCOX1F and DinoCOX1R from Lin et al. 2002) region. Positive bands were excised after gel electrophoresis (3% agarose) and purified using the QIAquick Gel Extraction Kit (Qiagen, Germantown, MD, USA). The purified product was then directly sequenced using ABI BigDye Terminator reagents and sequenced on an ABI 3100 Genetic Analyzer (Applied Biosystems, Foster City, CA, USA).

Phylogenetic analysis. The sequence results were aligned using BioEdit v7.0.9.0 (Hall 1999) and ClustalW (Thompson et al. 1994). The resulting alignments were improved manually, and ambiguously aligned regions were removed from further analyses. The SSU and LSU genes from 24 taxa (Table S1 in the supplementary material) were concatenated and analyzed using MP, ML, and BI to identify the taxa most closely related to *B. capitatum*. A smaller subset of nine taxa [*B. capitatum*, *K. bidigitata*, *K. brevis*, *K. mikimotoi*, *K. papilionacea*, *K. selliformis*, *Karlodinium veneficum* (D. L. Ballant.) J. Larsen (= *Karlodinium micrum*; Bergholtz et al. 2005), *Takayama acrotrocha*, and *Prorocentrum micans* Ehrenb.] was used to analyze each gene (SSU, LSU, ITS, *cox1*) independently as well as in a concatenated

four-gene data set. *P. micans* was used as an outgroup. Unweighted MP analysis was conducted in PAUP*4.0b10 (Swofford 2003). Heuristic searches of 100 random addition replicates with starting trees obtained by stepwise addition were followed by branch swapping utilizing tree bisection reconnection (TBR). ML analysis was also conducted in PAUP*4.0b10 (Swofford 2003). Branch support for MP was obtained from 1,000 bootstrap replicates, and branch support for ML was obtained from 100 bootstrap replicates. Substitution models for both ML and BI were obtained using MrModelTest2.3 (Nylander 2004). BI was conducted using MrBayes 3.1.2 (Ronquist and Huelsenbeck 2003). Markov chain Monte Carlo was run for 2 million generations with trees sampled every 100 cycles. The first 15,000 trees were discarded as the burn-in period, and posterior probabilities calculated from the remaining trees.

IFCB image analysis. Imaging FlowCytobot images of *Brachidinium* were automatically classified using the method of Sosik and Olson (2007) as in Campbell et al. (2010). All images classified as *Brachidinium* were manually checked, and misidentified images removed from the data set. The data were binned into 2 h intervals and used to calculate cell abundance and cell-size estimates for the duration of the recorded bloom period. Cell-size estimates were calculated directly from IFCB images. An individual cell's size estimate, determined from its cross-sectional area, was obtained by summing the number of image pixels remaining after removing the background pixels surrounding the cell. A background pixel color value was established for each image by averaging the pixel color values from the first column of the image. All images were grayscale, and pixel color values ranged from 0 (black) to 255 (white). The background pixel color range was created by extending the mean pixel color value $\sim 5\%$ in both directions (mean ± 15). A pixel was determined to be background if its color value fell within the background color range. Corner pixels were first added to a queue. Each pixel in the queue was evaluated, and if its color value fell within the background range, it was removed from the image. Once a pixel was evaluated, it was removed from the queue. All remaining pixels neighboring the removed pixel were then added to the queue. This process was repeated until the queue was empty. The remaining pixels (not the color values) were summed to produce an estimate of the cell size. All of the acquired images of *B. capitatum* were analyzed; these included images of cells in many different orientations. We also calculated the frequency of dividing cells and growth rate estimates as in Campbell et al. (2010). This information was coupled with current velocity data from the Texas Coastal Ocean Observation Network, Texas A&M University-Corpus Christi (<http://lighthouse.tamucc.edu/overview/109>) to determine whether cell abundance or cell size was related to tidal flows. Sunrise and sunset information was obtained from the United States Naval Observatory's Naval Oceanography Portal (<http://www.usno.navy.mil/USNO/astronomical-applications/data-services/data-services>).

RESULTS

Cell isolation. Ten individual cells were isolated from the water sample and measured. Cell widths ranged from 76 to 97 μm (mean: $83.5 \pm 5.7 \mu\text{m}$) including the lateral processes. Cell lengths ranged from 33 to 42 μm (mean: $36.5 \pm 3.0 \mu\text{m}$) including the ventral processes. Twenty-five additional cells from the same water sample were successfully isolated into five tubes for subsequent PCR amplification.

DNA extraction and amplification. Genetic sequences from the SSU, LSU, ITS, and *cox1* regions

were successfully obtained from extracted DNA of *K. bidigitata*, *K. papilionacea*, *K. selliformis*, *T. acrotrocha*, and whole genome amplification products from cells of *B. capitatum*. No variation among gene sequences from replicate tubes of *B. capitatum* was observed. All gene sequences obtained from *B. capitatum* were unique and not identical to any members of the *Karenia* genus. Sequences were deposited into GenBank, and accession numbers can be found in Table S1.

Phylogenetic analysis. Two equally parsimonious trees emerged from the concatenated SSU and LSU data set (2,053 nt) containing 24 taxa (Fig. 1). The best model selected by MrModelTest2.3 (Nylander 2004) was GTR+I+G (general time reversible with a portion of invariant sites and gamma rate distribution). Both equally parsimonious trees placed *B. capitatum* within the clade containing members of the genus *Karenia*. The ML and BI trees also placed *B. capitatum* within the clade containing the genus *Karenia* (data not shown). When all four genes in the reduced data set of nine taxa were analyzed independently (SSU: 1,684 nt, best model selected GTR+I; ITS: 528 nt, best model selected GTR+I+G; LSU: 613 nt, best model selected GTR+I+G; *cox1*:

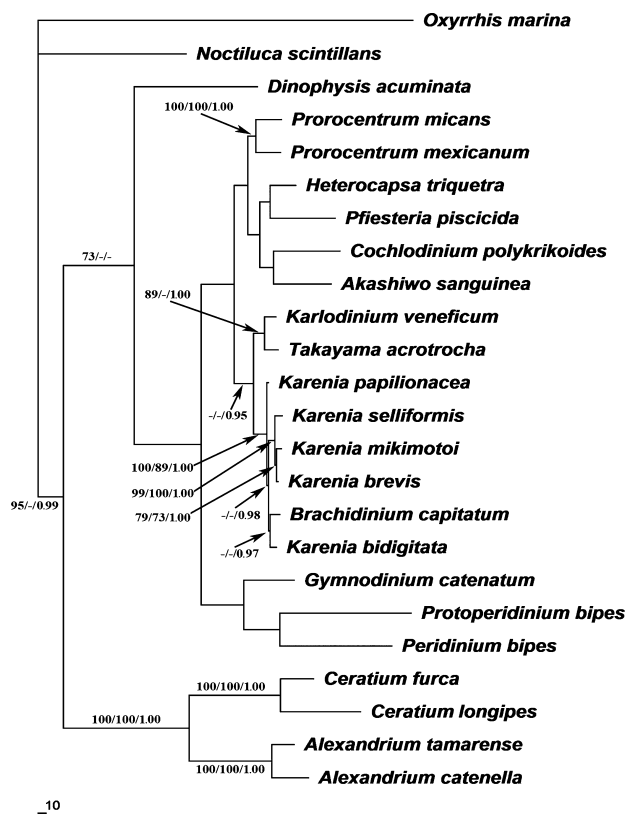


FIG. 1. One of two equally parsimonious (MP) trees of the SSU + LSU data set. Support values are maximum-parsimony bootstraps/maximum-likelihood bootstraps/Bayesian inference posterior probabilities. Only bootstrap values $>70\%$ and posterior probabilities >0.90 are shown. *Oxyrrhis marina* was used for the outgroup.

777 nt, best model selected GTR+G), *B. capitatum* was always placed within, or sister to, the clade containing members of the genus *Karenia* (Fig. 2, A–D). However, the exact placement of *B. capitatum* differed depending upon which gene was being analyzed. The most-parsimonious tree of the concatenated four-gene data set (Fig. 3) was identical in topology to the tree produced from the ML analysis (four-gene data set), while BI showed *K. bidigitata* and *K. papilionacea* as a sister clade to *B. capitatum*, *K. brevis*, *K. mikimotoi*, and *K. selliformis* but with a low posterior probability (<0.60). Bootstrap values showed the inclusion of *B. capitatum* in the *Karenia* clade to be well supported. However, while BI posterior probabilities showed moderate support (0.92) for the final placement of *B. capitatum*, both

the MP (<60%) and ML (<60%) bootstrap values showed it to be weakly supported (Fig. 3).

IFCB image analysis. A total of 71,487 images of *B. capitatum* were obtained from the IFCB over a 19 d period of image sampling (26 Oct.–13 Nov.) and included 1,636 images of dividing cells. Image data for 2 d (4 Nov., 8 Nov.) were unavailable. We were also unable to observe the end of the bloom due to technical difficulties with the IFCB. The maximum observed cell concentration was ~65 cells · mL⁻¹ (Fig. 4), and cell concentrations appeared to increase with the incoming tides, which suggested an offshore bloom origin. Cells of *B. capitatum* showed a high degree of morphological variability consistent with previous observations (Fig. 5). The cells' four major processes were observed in a

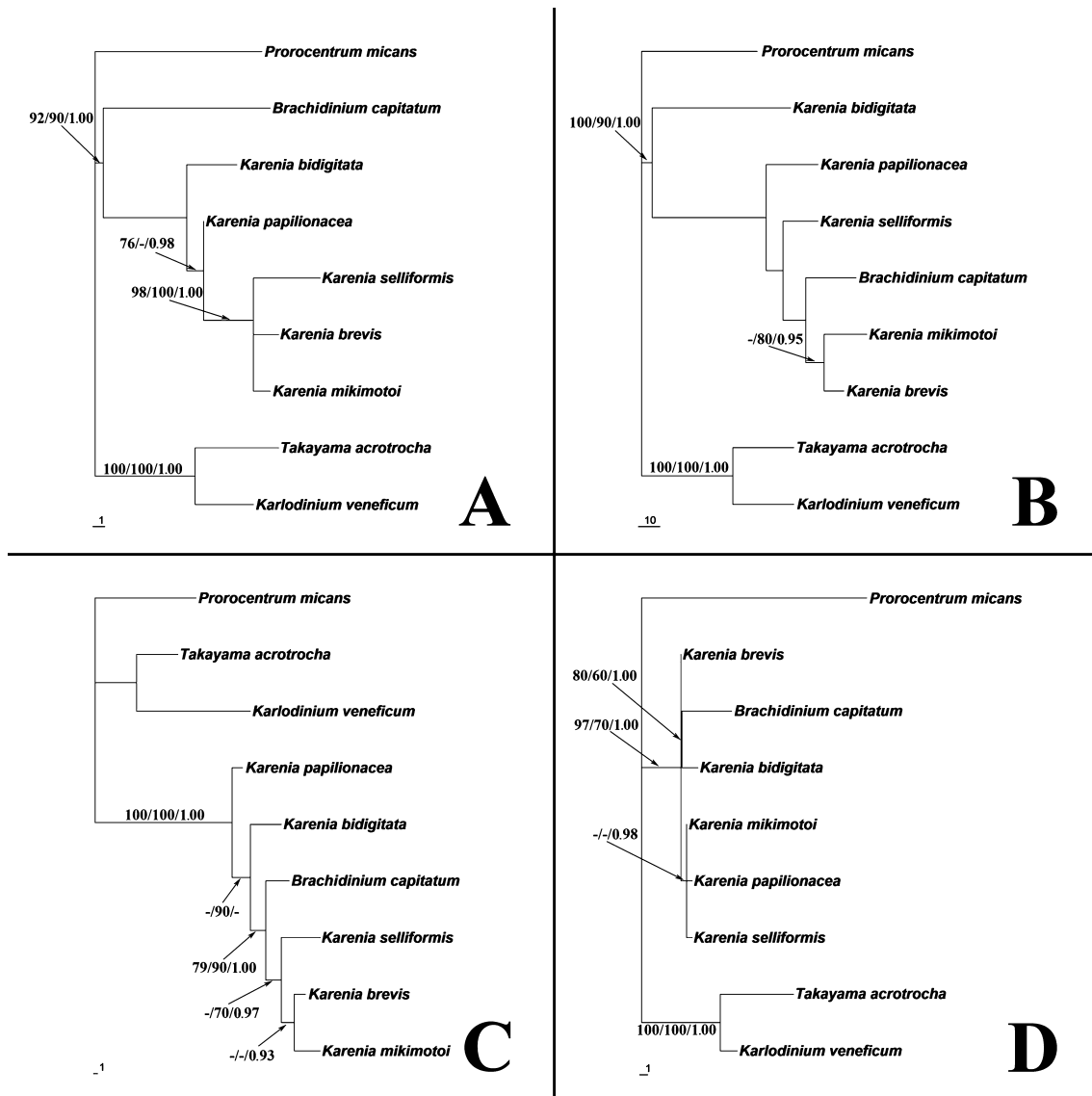


FIG. 2. The most-parsimonious tree for the SSU (A), ITS (B), LSU (C), and *cox1* (D) data sets. Support values are maximum-parsimony bootstraps/maximum-likelihood bootstraps/Bayesian inference posterior probabilities. Only bootstrap values >70% and posterior probabilities >0.90 are shown.

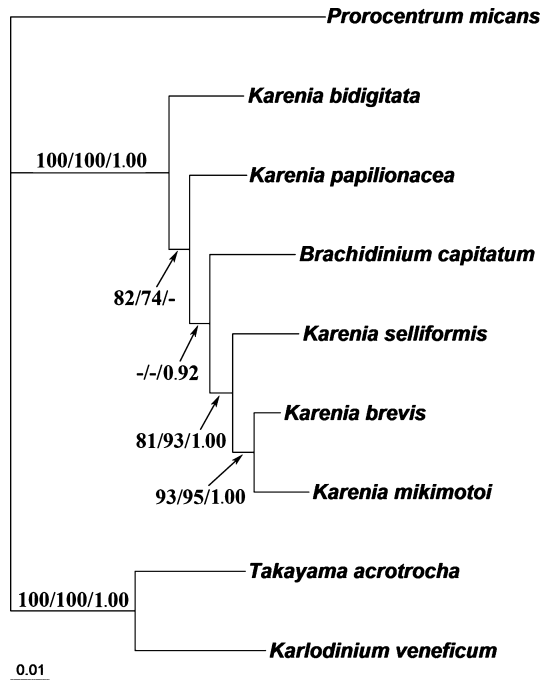


FIG. 3. Maximum-likelihood tree of the concatenated four-gene data set containing nine taxa. Support values are maximum-parsimony bootstraps/maximum-likelihood bootstraps/Bayesian inference posterior probabilities. Only bootstrap values >70% and posterior probabilities >0.90 are shown.

variety of orientations and appeared to be quite flexible. Orientation of the major processes did not appear to coincide with the time of day or tidal fluctuations (data not shown). Dividing cells were observed predominantly (>95%) between the hours of 18:00 and 06:00 local time, and ~46% were observed between the hours of 2:00 and 5:00 local time (Fig. 6). The numerous images of dividing cells allowed us to observe cells in various stages of

cell division (Fig. 7). Cell division did appear to be phased and allowed us to calculate the growth rate using the f_{\max} method. The maximum frequency of cell division was calculated to be 0.24 (2 Nov.), which yielded a growth rate estimate of 0.22 d^{-1} . As cultures of *B. capitatum* are not available, the duration of the terminal division event could not be determined, so we were unable to calculate growth rate using the mitotic index method. Average cell size showed a diel pattern of variation, with the largest average cell size observed immediately preceding the dark period and the smallest average cell size observed near the transition to the light period (Fig. 8). A reduced average cell size (~15% smaller than the maximum observed average cell size) was observed at ~5:00–6:00 local time daily and coincided with the termination of observed dividing cells and the onset of the light period.

DISCUSSION

The continuous sampling and imaging capabilities of the IFCB provided information that permitted study of a bloom of *B. capitatum*, a rare, typically oceanic dinoflagellate that otherwise may have gone unnoticed. Phylogenies based solely on morphological features have resulted in ambiguity regarding the placement of this group among the dinoflagellates and the paucity of observations has probably contributed to this ambiguity. *B. capitatum* cells isolated from a field sample taken during this 2007 bloom yielded the first-known genetic sequences from *B. capitatum* and permitted the first phylogenetic analysis of the genus to be conducted.

Species determination. *B. capitatum* cells have a unique external morphology consisting of four major processes extending from the cell body. Cells isolated from our water sample, and the IFCB

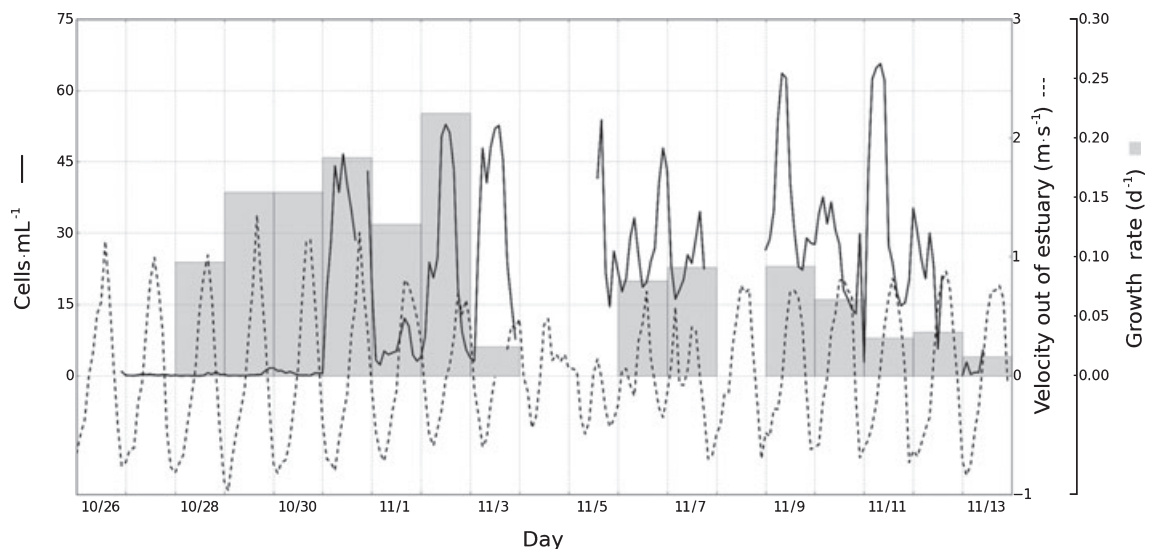


FIG. 4. Bihourly resolved *Brachidinium capitatum* cell concentration (solid line) and tide velocity (dashed line) over the 19 d period of image sampling. Negative values for tide velocity indicate an incoming tide. Gray bars represent the growth rate calculated using the f_{\max} method.

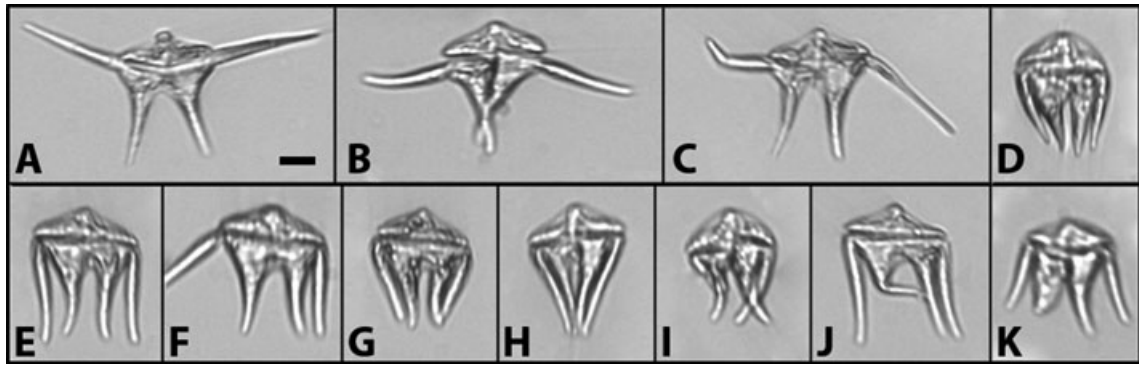


FIG. 5. Imaging FlowCytobot images of *Brachidinium capitatum* depicting the various position of the cells' four processes. (A) Normal cell with four processes extended. (B) Ventral processes crossed. (C, J) One process bent. (D, K) Ventral processes with different shapes. (E) Lateral processes parallel to ventral processes. (F) One lateral process extended. (G, H, I) Lateral processes compressed against, or crossing behind, ventral processes. Scale bar, 10 μm .

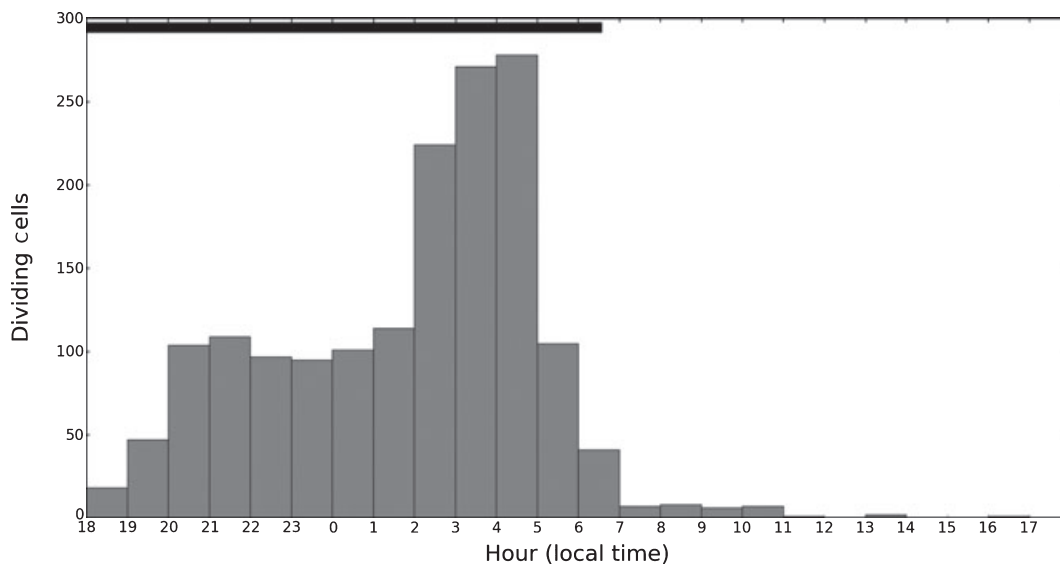


FIG. 6. Cumulative (entire bloom) occurrence of dividing cells as a function of time of day. Dividing cells were mainly observed during the dark period (indicated by the dark bar across the top).

images, all had this same basic external morphology. Measurements of cell length and width were larger than those reported for *B. brevipes* and *B. taylorii*. Cell length, however, did fall within the ranges of both *B. capitatum* and *B. catenatum*. While mean cell width was smaller than the range given in the original species description of *B. capitatum* (95–123 μm ; Taylor 1963), Gomez (2006) measured 29 cells, ranging in width from 65 to 130 μm (mean 98.4 + 27.1 μm), and described them all as being *B. capitatum*. The widths of our measured cells fell within this extended range. All cells in our water sample were observed as single or dividing cells, and no chains of cells were found. Size information coupled with external morphology supported the conclusion that the cells observed, and isolated for DNA sequencing, were all *B. capitatum*.

There appears to be some confusion surrounding the spelling of the genus *Brachidinium*. The original

spelling of the genus *Brachydidinium* (Taylor 1963) was corrected to *Brachidinium* by Taylor (1966), who stated the original spelling was an “etymological” error, with the prefix intended to mean “armed” rather than “wide.” Sournia (1973) declared this to be an illegitimate correction and reinstated the original spelling, *Brachydidinium*. Yet, the correction to *Brachidinium* is adopted by AlgaeBase, an online database of worldwide algal species (Guiry and Guiry 2010). We have chosen to use the corrected genus name, *Brachidinium*, but note that both spelling variants continue to be used (Gomez 2006, Taylor et al. 2008).

Phylogenetic analysis. The SSU+LSU tree (Fig. 1) contains members of several major branches of dinoflagellates, including the Dinophysiales, Gonyaulacales, Gymnodiniales, Peridiniales, and Procentrales. A wide range of dinoflagellate taxa were included to reduce the chance of biasing the result toward previous morphology based relationships

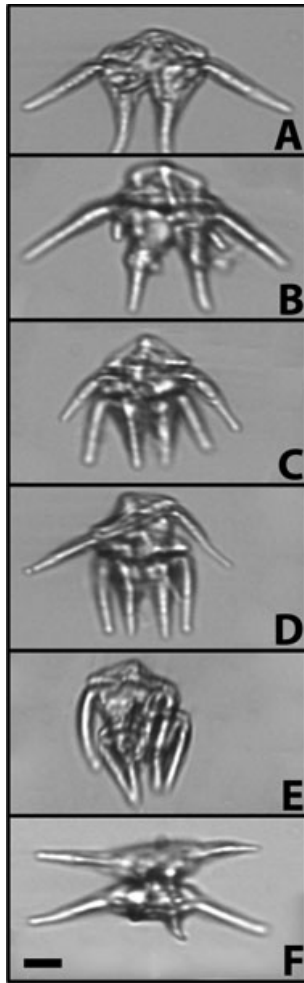


FIG. 7. Hypothesized sequence of division in *Brachidinium capitatum*. (A) A single cell. (B) A cell beginning the division process. Two smaller processes can be seen extending from under the lateral processes. (C, D, E) Cells in intermediate stages of division. (F) Ventral view of two cells completing the division process. Scale bar, 10 μm .

(Gomez et al. 2005a). The placement of *B. capitatum* within the genus *Karenia* was well supported in all analyses. This result was not unexpected as some morphological features of *B. capitatum* have been previously found to be very similar to *K. papilionacea* (Gomez et al. 2005a). Our results show, however, that genetically *B. capitatum* is more closely related to *K. bidigitata*. To better constrain the correct placement of *B. capitatum*, a smaller subset of nine taxa was used to construct a concatenated four-gene phylogeny. In addition to several *Karenia* spp., *Karlodinium veneficum* and *T. acrotrocha* were included due to their membership in the Kareniaceae (Bergholtz et al. 2005) and close phylogenetic relationship with the genus *Karenia* (Daugbjerg et al. 2000, Haywood et al. 2004, Bergholtz et al. 2005). The combined four-gene phylogeny (Fig. 2) shows a slightly different tree topology within the genus *Karenia* when compared to the SSU+LSU tree (Fig. 1). *B. capitatum* appears as a sister to the

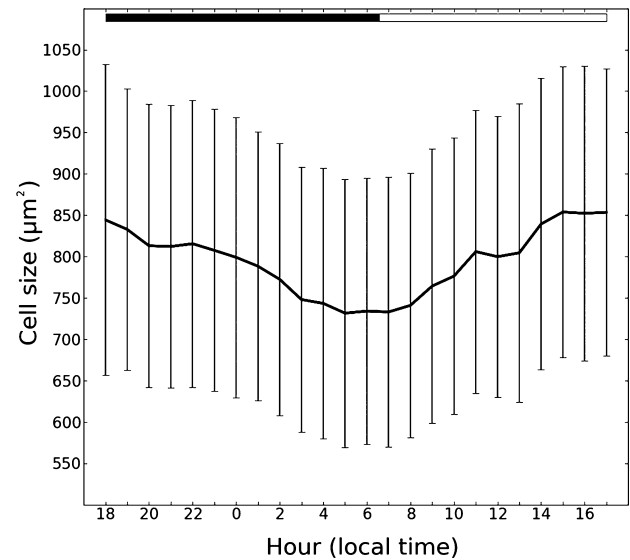


FIG. 8. Hourly average size (cross-sectional area) for all cells observed over the 19 d period of image sampling. Dark period indicated by black bar at the top. Error bars indicate one standard deviation from the mean.

clade containing *K. brevis*, *K. mikimotoi*, and *K. selliformis*. This placement was moderately supported by the BI (post. prob. >0.90), but did not have strong bootstrap support (<60% for both ML and MP; Fig. 3). While the topology of the genus *Karenia* (including *B. capitatum*) differed among genes, *B. capitatum* was always more closely related to members of the genus *Karenia* than to either *K. veneficum* or *T. acrotrocha* (Fig. 2, A–D). These results provide support for the membership of *B. capitatum* in the Kareniaceae, but its placement within the genus *Karenia* and the validity of the genus *Brachidinium* remain uncertain.

The suggestion by Gomez et al. (2005a) based on morphological similarities that the genus *Karenia* is a possible synonym of *Asterodinium-Brachidinium* is supported by our phylogenetic analyses. (Note: *Asterodinium* is the only other genus in the Brachidiniaceae. We did not observe any specimens representing the genus *Asterodinium* and therefore cannot provide insight with any certainty about its phylogenetic relationships.) Notably, however, all four-gene sequences of *B. capitatum* were unique and did not match any other known sequences, precluding the possibility of *B. capitatum* being an oceanic life-history stage of *K. papilionacea* as proposed in Gomez (2006).

The close phylogenetic relationship with the genus *Karenia* raises the question of whether *B. capitatum* might be a toxin-producing species. Other members of the genus *Karenia*, particularly *K. brevis* and *K. mikimotoi*, are known to produce toxins capable of killing fish (Neely and Campbell 2006, Errera et al. 2010), and the observed concentrations of *B. capitatum* during this bloom are well above levels that are cause for concern in *K. brevis* (Heil and Steidinger 2008). We were unable to conduct a toxin

analysis due to the lack of live specimens, and it remains unknown whether *B. capitatum* is capable of toxin production.

IFCB image analysis. The number of *B. capitatum* cells observed in this study (~70,000) far exceeds previous studies (17 cells in Gomez et al. 2005b, 29 cells in Gomez 2006). Most cells were similar in appearance to the one live cell observed by Gomez et al. (2005b). While individual cell morphology was highly variable (Fig. 5), the lack of nucleotide differences in gene sequences among replicates of *B. capitatum* suggests that the bloom was monospecific. This result was also supported by single-cell sequencing of the LSU rDNA (results not shown). Morphological variability coupled with the lack of genetic differences among cells of *B. capitatum* support the idea that other described species of *Brachidinium* may simply be morphological variants of *B. capitatum* (Gomez et al. 2005b).

Dividing cells of *B. capitatum* were predominantly observed during the dark period (Fig. 6) with a peak in dividing cells observed ~2 h before dawn, earlier than that observed for another dinoflagellate species, *Dinophysis* cf. *ovum*, that bloomed in the same geographic area 4 months later (Campbell et al. 2010). A majority of dividing *Dinophysis* cf. *ovum* cells were observed within a 3 h period occurring 7–10 h after local midnight, which is just after the onset of the light period (Campbell et al. 2010). Cell division just before dawn has been previously observed, however, in cultures of two other dinoflagellate species, *Ceratium furca* and *C. fusus* (Baek et al. 2009). When maintained under a 12:12 light:dark cycle similar to our observed field conditions, both species completed cell division before the onset of the light period, and the highest percentage of dividing cells was observed ~1 h before the light period (Baek et al. 2009).

The phased cell division in *B. capitatum* allowed us to estimate daily growth rate during the bloom. The f_{\max} growth rate calculation produced a maximum estimate of 0.22 d^{-1} (Fig. 4). It should be noted that the f_{\max} method used here can produce an underestimate of the growth rate if the duration of mitosis is less than the sampling interval (McDuff and Chisholm 1982). Since very little information is currently known about *B. capitatum*, we cannot state with any certainty the duration of mitosis. The estimated growth rate is not unreasonable for an oceanic dinoflagellate and is similar to the maximum rate (0.26 d^{-1}) estimated for *Dinophysis* at the same location 4 months later (Campbell et al. 2010). Members of the genus *Karenia* appear to be the closest related species to *B. capitatum* and provide another useful comparison. The average specific growth rate observed for *K. brevis* during 10 research cruises was 0.23 d^{-1} (Van Dolah et al. 2008), which is similar to our value of 0.22 d^{-1} for *B. capitatum*.

The imaging capability of the IFCB also allowed the extraction of information about cell-size varia-

tion over time. For the natural population of *B. capitatum*, cell-size variation showed a diel pattern (Fig. 8) similar to that seen in other phytoplankton species, including *Amphidinium operculatum* (Leighfield and Van Dolah 2001), *Micromonas pusilla* (DuRand et al. 2002), and *K. brevis*, a close phylogenetic relative (Van Dolah et al. 2008). Continuous sampling by IFCB provides a very large number of quantitative cell-size measurements at sufficient frequency that it is possible to resolve diel patterns for individual species. The potential to use these patterns in cell size for estimates of species-specific growth rate (Sosik et al. 2003) is an important new advantage of IFCB data.

CONCLUSION

The information presented here provides insight into the life cycle of a rare oceanic dinoflagellate. We have shown that, even though typically observed in low numbers in oceanic environments, *B. capitatum* is capable of producing blooms, and that actively growing cells can be transported into estuarine waters. The full impacts of this species, particularly concerning toxin production, remain to be studied. The combination of morphological features similar to the genus *Karenia* and a phylogenetic analysis placing *B. capitatum* in the *Karenia* clade leads us to propose moving the genus *Brachidinium* into the Kareniaceae. However, the lack of agreement among individual gene phylogenies suggests that the inclusion of different genes and more members of the genus *Karenia* are necessary before a final determination regarding the validity of the genus *Brachidinium* can be made.

This work was supported by NOAA ECOHAB award NA06NOS4780244 to L. C. and J. R. Gold, and CICEET award 07025 to H. M. S., R. J. O., and L. C. We thank the Cawthron Institute Collection of Micro-algae (CICCM) for providing the sample cultures of *Karenia* spp., Raffaele Siano for providing the culture of *T. acrotrocha*, and C. Hyatt for sample collection. We also thank A. W. Lievens and P. C. Silva for helpful advice regarding the spelling of the genus *Brachidinium*. This article is ECOHAB contribution number 612.

- Baek, S. H., Shimode, S., Shin, K., Han, M. & Kikuchi, T. 2009. Growth of dinoflagellates, *Ceratium furca* and *Ceratium fusus* in Sagami Bay, Japan: the role of vertical migration and cell division. *Harmful Algae* 8:843–56.
- Bergholtz, T., Daugbjerg, N., Moestrup, Ø. & Fernandez-Tejedor, M. 2005. On the identity of *Karlodinium veneficum* and description of *Karlodinium armiger* sp. nov. (Dinophyceae), based on light and electron microscopy, nuclear-encoded LSU rDNA, and pigment composition. *J. Phycol.* 42:170–93.
- Campbell, L., Olson, R. J., Sosik, H. M., Abraham, A., Henrichs, D. W., Hyatt, C. J. & Buskey, E. J. 2010. First harmful *Dinophysis* (Dinophyceae, Dinophysiales) bloom in the U.S. is revealed by automated imaging flow cytometry. *J. Phycol.* 46:66–75.
- Daugbjerg, N., Hansen, G., Larsen, J. & Moestrup, Ø. 2000. Phylogeny of some of the major genera of dinoflagellates based on ultrastructure and partial LSU rDNA sequence data, including the erection of three new genera of unarmoured dinoflagellates. *Phycologia* 39:302–17.

- Doyle, J. J. & Doyle, J. L. 1990. A rapid total DNA isolation procedure for fresh plant tissue. *Focus* 12:13–5.
- DuRand, M. D., Green, R. E., Sosik, H. M. & Olson, R. J. 2002. Diel variations in optical properties of *Micromonas pusilla* (Prasinophyceae). *J. Phycol.* 38:1132–42.
- Elwood, H. J., Olsen, G. J. & Sogin, M. L. 1985. The small-subunit ribosomal RNA gene sequences from the hypotrichous ciliates *Oxytricha nova* and *Stylonychia pustulata*. *Mol. Biol. Evol.* 2:399–410.
- Errera, R. M., Bourdelais, A., Drennan, M. A., Dodd, E. B., Henrichs, D. W. & Campbell, L. 2010. Variation in brevetoxin and brevetoxin content among clonal cultures of *Karenia brevis* may influence bloom toxicity. *Toxicon* 55:195–203.
- Gomez, F. 2006. The dinoflagellate genera *Brachidinium*, *Asterodinium*, *Microceratium*, and *Karenia* in the open SE Pacific Ocean. *Algae* 21:445–52.
- Gomez, F., Nagahama, Y., Takayama, H. & Furuya, K. 2005a. Is *Karenia* a synonym of *Asterodinium-Brachidinium* (Gymnodinales, Dinophyceae)? *Acta Bot. Croat.* 64:263–74.
- Gomez, F., Yoshimatsu, S. & Furuya, K. 2005b. Morphology of *Brachidinium capitatum* F.J.R. Taylor (Brachidinales, Dinophyceae) collected from the western Pacific Ocean. *Cryptogam. Algal.* 26:165–75.
- Guiry, M. D. & Guiry, G. M. 2010. *Algaebase*. World-wide electronic publication, National University of Ireland, Galway. Available at: <http://www.algaebase.org> (last accessed 10 August 2010).
- Hall, T. A. 1999. BioEdit: a user-friendly biological sequence alignment editor and analysis program for Windows 95/98/NT. *Nucleic Acids Symp. Ser.* 41:95–8.
- Haywood, A. J., Steidinger, K. A., Truby, E. W., Bergquist, P. R., Bergquist, P. B., Adamson, J. & MacKenzie, L. 2004. Comparative morphology and molecular phylogenetic analysis of three new species of the genus *Karenia* (Dinophyceae) from New Zealand. *J. Phycol.* 40:165–79.
- Heil, C. A. & Steidinger, K. A. 2008. Monitoring, management, and mitigation of *Karenia* blooms in the eastern Gulf of Mexico. *Harmful Algae* 8:611–7.
- Henrichs, D. W., Renshaw, M. A., Santamaria, C. A., Richardson, B., Gold, J. R. & Campbell, L. 2008. PCR amplification of microsatellites from single cells of *Karenia brevis* preserved in Lugol's iodine solution. *Mar. Biotechnol.* 10:122–7.
- Hernandez-Becerril, D. U. & Bravo-Sierra, E. 2004. New records of planktonic dinoflagellates (Dinophyceae) from the Mexican Pacific Ocean. *Bot. Mar.* 47:417–23.
- Leighfield, T. A. & Van Dolah, F. M. 2001. Cell cycle regulation in a dinoflagellate, *Amphidinium operculatum*: identification of the diel entraining cue and a possible role for cyclic AMP. *J. Exp. Mar. Biol. Ecol.* 262:177–97.
- Lin, S. J., Zhang, H. A., Spencer, D. F., Norman, J. E. & Gray, M. W. 2002. Widespread and extensive editing of mitochondrial mRNAs in dinoflagellates. *J. Mol. Biol.* 320:727–39.
- McDuff, R. E. & Chisholm, S. W. 1982. The calculation of *in situ* growth rates of phytoplankton populations from fractions of cells undergoing mitosis: a clarification. *Limnol. Oceanogr.* 27:783–8.
- Medlin, L., Elwood, H. J., Stickel, S. & Sogin, M. L. 1988. The characterization of enzymatically amplified eukaryotic 16S-like rRNA-coding regions. *Gene* 71:491–9.
- Neely, T. & Campbell, L. 2006. A modified assay to determine hemolytic toxin variability among *Karenia* clones isolated from the Gulf of Mexico. *Harmful Algae* 5:592–8.
- Nylander, J. A. A. 2004. *MrModelTest v2*. Program distributed by the author. Evolutionary Biology Centre, Uppsala University, Uppsala, Sweden.
- Olson, R. J. & Sosik, H. M. 2007. A submersible imaging-in-flow instrument to analyze nano- and microplankton: Imaging FlowCytobot. *Limnol. Oceanogr. Methods* 5:195–203.
- Ronquist, F. & Huelsenbeck, J. P. 2003. MrBayes 3: Bayesian phylogenetic inference under mixed models. *Bioinformatics* 19:1572–4.
- Scholín, C. A., Herzog, M., Sogin, M. & Anderson, D. M. 1994. Identification of group- and strain-specific genetic markers for globally distributed *Alexandrium* (Dinophyceae). II. Sequence analysis of a fragment of the LSU rRNA gene. *J. Phycol.* 30:999–1011.
- Sosik, H. M. & Olson, R. J. 2007. Automated taxonomic classification of phytoplankton sampled with imaging-in-flow cytometry. *Limnol. Oceanogr. Methods* 5:204–16.
- Sosik, H. M., Olson, R. J., Neubert, M. G. & Shalapyonok, A. 2003. Growth rates of coastal phytoplankton from time-series measurements with a submersible flow cytometer. *Limnol. Oceanogr.* 48:1756–65.
- Sournia, A. 1972. Une période de poussées phytoplanctoniques près de Nosy-Bé (Madagascar) en 1971. *Cah. ORSTOM Ser. Oceanogr.* 10:151–9.
- Sournia, A. 1973. Catalogue des espèces et taxons infraspécifiques de Dinoflagellés marins actuels publiés depuis la révision de J. Schiller. I. Dinoflagelles libres. *Nova Hedwigia Beih.* 48:1–92.
- Sournia, A. 1986. *Atlas du Phytoplancton Marin. Volume 1: Cyanophytes, Dictyochophycées, Dinophycées et Raphidophycées*. Editions du Centre National de la Recherche Scientifique, Paris, 219 pp.
- Swofford, D. L. 2003. *PAUP* Phylogenetic Analysis Using Parsimony (*and Other Methods) v4.0b10*. Sinauer Associates, Sunderland, Massachusetts.
- Taylor, F. J. R. 1963. *Brachidinium*, a new genus of the Dinococcales from the Indian Ocean. *J. S. Afr. Bot.* 29:75–8.
- Taylor, F. J. R. 1966. Phytoplankton of the south western Indian Ocean. *Nova Hedwigia* 12:433–76.
- Taylor, F. J. R., Hoppenrath, M. & Saldarriaga, J. F. 2008. Dinoflagellate diversity and distribution. *Biodivers. Conserv.* 17:407–18.
- Thompson, J. D., Higgins, D. G. & Gibson, T. J. 1994. Clustal-W - improving the sensitivity of progressive multiple sequence alignment through sequence weighting, position-specific gap penalties and weight matrix choice. *Nucleic Acids Res.* 22:4673–80.
- Van Dolah, F. M., Leighfield, T. A., Kamykowski, D. & Kirkpatrick, G. J. 2008. Cell cycle behavior of laboratory and field populations of the Florida red tide dinoflagellate, *Karenia brevis*. *Continental Shelf Res.* 28:11–23.
- White, T. J., Bruns, T., Lee, S. & Taylor, J. 1990. Amplification and direct sequencing of fungal ribosomal RNA genes for phylogenetics. In Innis, M. A., Gelfand, D. H., Sninsky, J. J. & White, T. J. [Eds.] *PCR Protocols: A Guide to Methods and Applications*. Academic Press, San Diego, pp. 315–22.

Supplementary Material

The following supplementary material is available for this article:

Table S1. Accession numbers used in phylogenetic analyses.

This material is available as part of the online article.

Please note: Wiley-Blackwell are not responsible for the content or functionality of any supporting materials supplied by the authors. Any queries (other than missing material) should be directed to the corresponding author for the article.